UNIT-I
Sources of Radiation (from Smith)

1.1 Introduction

The radiation to which humans are exposed varies widely in :

- type and energy distribution,
- geographical distribution, and with
- occupation.

The main sources of radiation can be categorized as follows :

Category	Source/Machine	Radiation
Environmental	Cosmic Rays	neutrons, protons, electrons, photons
	Radioactivity	α- and β- particles, γ-rays, neutrons
Artificial	orthovoltage X-rays	kV X-rays
	linac/betatron	MV X-rays, electrons and radioactivity
	Van de Graaff and Cyclotron	protons, neutrons and radioactivity
	Synchrotron	electrons, protons, X-rays, uv photons
	Nuclear Reactor	neutrons, γ-rays, residual radioactivity

The minimum requirements for a full understanding of radiation action are :

- the energy spectrum of the incoming radiation,
- the energy-dependent cross-sections of the medium,
- the density and atomic number of the medium.

This chapter considers the energy spectra from some of the most important sources of radiation and, in the case of artificial sources, its dependence on the means of production. In the consideration of background radiation, Table (1.1) shows that there are contributions from both natural and man-made sources.

The natural environment accounts for ~ 80% of the radiation exposure of the UK population. Of this, α-particle emissions from atmospheric radon are by far the most important. Some building materials contain long-lived actinide elements in small quantities while traces of naturally occurring isotopes (^{40}K and ^{12}C) are present in all of us. More detailed figures are given in Chapter 11.

Table (1.1) Terrestrial sources of radiation averaged over the UK population [1]. The unit of exposure (μSv yr^{-1}) is defined in section 7.1. Large differences from these means are received by certain population groups (see chapter 11). Data for 1994 come from [1] in chapter 11.

Category	Main source	1986	1994
nuclear power	^{235}U fission products, ^{90}Sr,^{137}Cs	2	0.4
occupational exposure	X-rays, isotopes	8	7
weapons tests	^{235}U, ^{239}Pu fission products	10	5
everyday sources	coal, tobacco, air travel	10	0.4
medical tests	X-rays, radioisotope scans	250	370
cosmic rays	protons, electrons, neutrons	300	260
food	^{40}K, ^{137}Cs, ^{14}C,^{131}I	370	300
rocks and buildings	^{238}U, ^{235}U, ^{232}Th	400	350
atmosphere	^{222}Rn,^{137}Cs	800	1300
TOTAL		2150	2593

1.2 Cosmic Rays

Cosmic rays span a very wide range of energies (keV to GeV) and include charged particles as high in mass as the transition elements. From the radiation protection point of view, the most important are likely to be neutrons, electrons and protons (terrestrial cosmic rays). These are the consequence of interactions of primary cosmic rays with the earth's atmosphere. They span an approximate energy range from keV to MeV and are important at altitudes from sea level up to the height of commercial air travel.

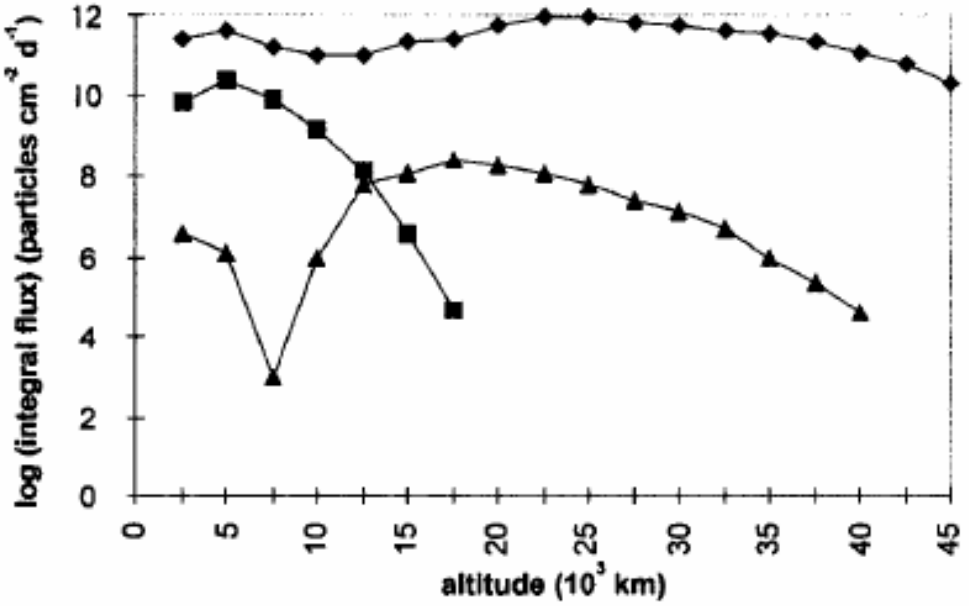

Fig. (1.1) Estimated log(integral flux) of electrons and protons versus altitude above mean sea level (MSL) in the equatorial plane. Units are particles cm^{-2} day^{-1}. Data taken from [2].
◆ electrons > 0.5 MeV ■ protons > 10 MeV ▲ electrons > 4 MeV. Approximate fluxes at MSL are : neutrons 0.01 cm^{-2} s^{-1} MeV^{-1}, muons 0.009 cm^{-2} s^{-1} sr^{-1}, electrons 0.002 cm^{-2} s^{-1} sr^{-1}, protons 0.0002 cm^{-2} s^{-1} sr^{-1} [3].

At higher altitudes the very high fluxes of energetic charged particles, Fig. (1.1), may well affect the instrumentation required for satellite and space exploration. These cosmic rays are both galactic and solar in origin, the latter showing a variation due to the occurrence of solar flares.

Galactic and solar cosmic rays are affected by the earth's magnetic field. This gives rise to the radiation belts with the features known as the *polar horns* and the *South Atlantic anomaly*.

1.3 Radioactive Sources

Radioactive decay is the process by which a nucleus in an unstable state is able to

achieve greater stability by emitting a particle or photon.

The probability per second that the emission takes place is the decay constant. If there are N_0 nuclei present originally (at time $t = 0$), then at a later time t, there will be :

$$N_t = N_0 \exp(-\lambda t)$$

The mean lifetime against decay is $\tau = 1/\lambda$. This is the average time for the number of radioactive nuclei to decrease by *1/e* (1/2.71828 = 0.36788). An alternative measure of this probability is the average time for the number of radioactive nuclei to halve. In this case, $N_t = N_0/2$, so $T_{1/2} = \ln 2/\lambda = 0.693/\lambda$.

The activity of a radioactive substance, *A*, is defined as the number of disintegrations per second, i.e. $A = N\lambda$. Therefore :

$$A_t = A_0 \exp(-\lambda t) \qquad (1.1)$$

and the unit of activity, the Becquerel (Bq) = 1 disintegration per second. The old unit is the Curie (Ci) which is the activity of 1g of radium = 3.7×10^{10} Bq. A convenient benchmark worth remembering is 100 μCi = 3.7 MBq.

At any one time, the number of radioactive atoms present is the product of the activity and the mean lifetime, i.e. $(N\lambda)\tau = N$.

1.3.1 *Beta decay*

The three forms of beta decay are β^- emission, β^+ emission and electron capture and they are called isobaric decay because the mass number of the nucleus does not change. The charge of the nucleus, Z, changes by ± 1.

$$n \rightarrow p + e^- + \bar{\nu}_e$$

$$p \rightarrow n + e^+ + \nu_e$$

$$p + e^- \rightarrow n + \nu_e$$

In β^- emission, the massive residual nucleus receives only a small fraction of the available kinetic energy. This means that energy is essentially conserved between the electron and the accompanying antineutrino. However, because of the presence of the residual nucleus, momentum need not be conserved between the two emitted particles – the electron and the antineutrino.

The energy spectrum for an allowed decay can be re-expressed from the expression for the momentum distribution, [4], as :

$$N(W)\,dW = \frac{|P|^2}{\tau_0} F(Z,W)\left(W^2 - 1\right)^{1/2}\left(W_0 - W\right)^2 W\,dW \qquad (1.2)$$

This gives the number of β particles emitted with an energy between W and $W+dW$ where W is the total electron energy normalized to the rest mass energy, ($W = (E_\beta/m_0c^2)+1$). W_0 is the total energy of the transition, $W_0 = (E_{\beta,max}/m_0c^2)+1$. The other three terms in this expression are :

- the square of the transition matrix element $|P|^2$. This represents the overlap of the nucleon wave functions of the initial state before the decay, and the final state after the decay has taken place. For allowed transitions this is of the order of unity.
- the Coulomb correction factor, $F(Z,W)$. This accounts for the force exerted on the emitted electron or positron when it is still within the vicinity of the nucleus. The deceleration of an electron produces more low energy β^- particles, and the acceleration of a positron fewer low energy β^+ particles than would otherwise be expected when their energies are measured at infinity. For the (unrealistic) case of Z=0, the function $F(Z,W)=1$.
- the β-decay constant, $\tau_0 = h^7/(64\pi^4 m_0^5 c^4 g^2)$ with a value of ≈ 7000 s. The precise value depends on the value of the Fermi constant, $g \approx 10^{-48}$ m^3 J.

The shape of Fig.(1.3) will alter as both the Coulomb correction factor and the square of the interaction matrix element depart from unity. In particular :

- when a realistic *F(Z,W)* is used for the ^{11}C spectrum, it will show fewer positrons emitted at low energies.
- for an allowed β^- emitter, the number of low energy particles will be enhanced. This means that the electron energy spectrum will not fall to zero at low energies.
- a change of shape also occurs when the decay becomes less allowed [4].

The decay constant is given by the integration of Eq.(1.2) over all energies :

$$\lambda = \frac{0.693}{T_{1/2}} = \int_1^{W_0} N(W)\, dW \qquad (1.3)$$

1.3.2 Gamma decay

When a nucleus de-excites by the emission of γ-radiation, the energy spectrum will be discrete since it is governed by transitions between quantized nuclear energy levels.

The selection rules which govern these transitions are determined by the spins and parities of the levels involved. For levels having energies and spins E_0, I_0 and E_1, I_1 the energy of the emission is :

$$h\nu = E_1 - E_0 \tag{1.4}$$

while the change in angular momentum is :

$$\Delta I = I_1 - I_0 \leq \ell \leq I_1 + I_0 \tag{1.5}$$

where ℓ is the non-zero angular momentum carried away by the emitted photon.

The multipolarity of the radiation is 2^ℓ such that $\ell = 0,1,2\ldots$ corresponds to monopole, dipole, quadrupole.... radiation respectively. However, transitions are prohibited between states having $I_1 = I_0 = 0$. This is because the transverse nature of electro-magnetic radiation prohibits the emission of an $\ell = 0$ monopole.

A distinction is made between electric and magnetic radiation on the basis of the parity change, $\Delta\pi$. Electric radiation corresponds to a change of $(-1)^\ell$ and magnetic radiation to $-(-1)^\ell$. Thus, for a transition between levels in which there is no change in parity, ℓ can only be 0 or even for electric radiation and odd for magnetic radiation.

An approximate relation between the energy of electric radiation and the probability of its emission is given by [5] :

$$\lambda_{el} = \frac{1}{\tau_{el}} = S\,\frac{2\pi\nu}{137}\left(\frac{R}{\lambda\!\!\!^{-}}\right)^{2\ell} \tag{1.6}$$

for a nucleus of mass number A and radius $R=R_0 A^{1/3}$ ($R_0 = 1.20 \pm 0.03$ fm is the nuclear unit radius). S is a statistical factor [4] given by :

$$S = \frac{2(\ell+1)}{\ell\left[1 \times 3 \times 5 \ldots (2\ell+1)\right]^2}\left(\frac{3}{\ell+3}\right)^2 \qquad (1.7)$$

Since the probability of a transition is proportional to S, it decreases rapidly as ℓ becomes larger than unity.

For the same multipolarity, the probability of a magnetic transition is smaller by a factor of about 10.

$$\frac{\tau_m}{\tau_{el}} \approx 4.4 \times A^{2/3} \qquad (1.8)$$

In Fig.(1.4) the difference in spin of the 171keV transition is unity, with no parity change. The most likely emission is therefore M1 with a small admixture of E2. Even though an ℓ =2 transition is less likely than ℓ = 1 by a factor of 210, Eq.(1.7), an electric transition of the same angular momentum is more likely by a factor of 102, Eq.(1.8).

A difference in the relative probabilities of 102/210 is not sufficiently small to make the decay pure M1 in character. Since these arguments work the other way when ℓ =2 with no parity change, the 245 keV line is pure E2.

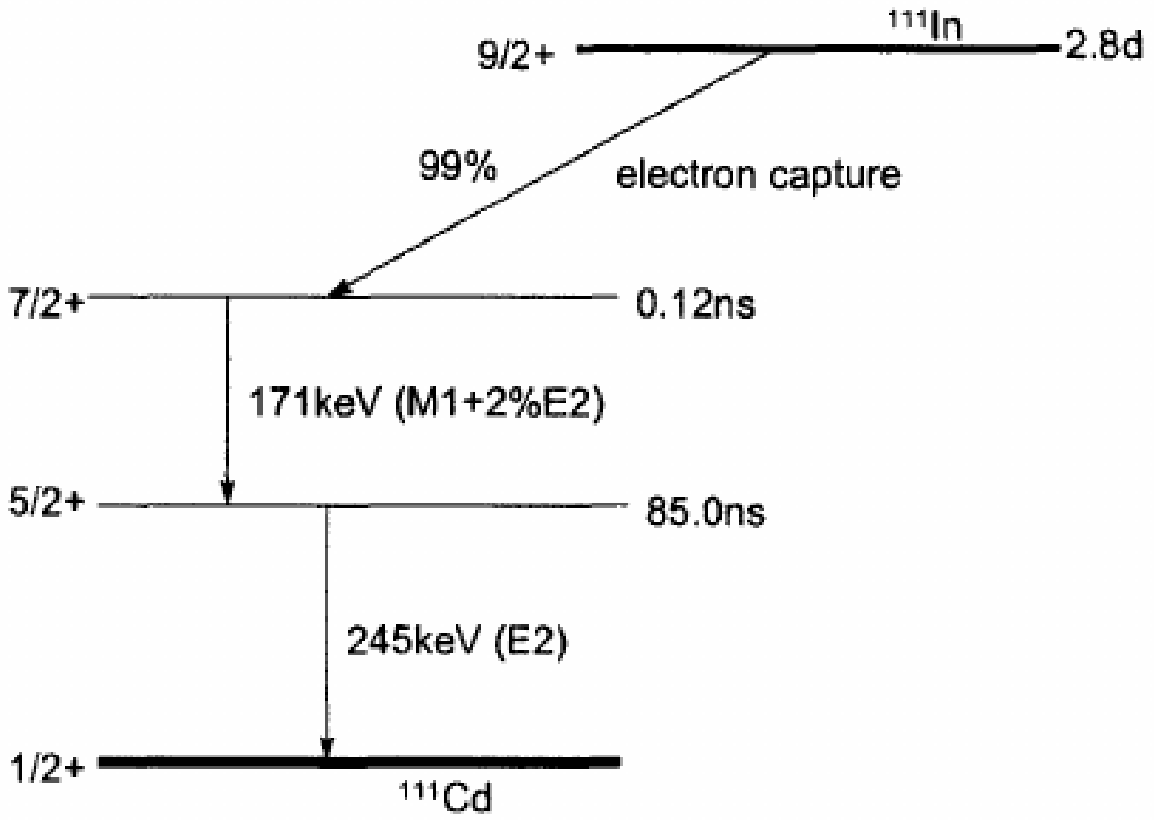

Fig.(1.4) Partial decay scheme of ^{111}In.

1.3.3 *Alpha decay*

The emissions from α-decay are also discrete in energy. Being an assembly of 2 protons and 2 neutrons, the energetics of α-particle emission can be understood initially using the semi-empirical mass formula [4]. This gives the total mass of a nucleus in terms of the number of protons and neutrons. Neglecting any electronic binding energy :

$$M(Z,A) = Zm_p + (A-Z)m_n - k_v A + k_s A^{2/3} + k_c Z^2 / A^{1/3} + k_a (A-2Z)^2 / A \pm \delta \tag{1.9}$$

where k_v, k_s, k_c, k_a and δ are called the volume, surface, Coulomb, asymmetry and pairing constants. The binding energy of the nucleus *M(Z,A)* is the sum of the last five terms in Eq.(1.9).

Energy released when a parent nucleus, mass number *A* and charge number *Z*, decays to a daughter of mass *A - 4* and charge *Z - 2*, is :

$$Q = M(Z,A) - M(Z-2,A-4) - M(^4He) \tag{1.10}$$

where *M(Z,A)* is the mass of the parent nucleus.

Substitution of Eq.(1.9) into Eq.(1.10), and using 28.3 MeV for the binding energy of the ^{4}**He** nucleus, gives the α-decay energy. This can be written :

$$E_\alpha = 28.3 - 4k_v + \frac{8}{3}\frac{1}{A^{1/3}} k_s + 4k_c \frac{Z}{A^{1/3}}\left(1 - \frac{Z}{3A}\right) - 4k_a\left(1 - \frac{2Z}{A}\right)^2 \tag{1.11}$$

Eq.(1.11) applies to ground-state to ground-state transitions between parent and daughter nuclei. In this transition Z and A refer to the mean values of the two nuclei. A transition which involves an excited state of either of the nuclei will add to, or subtract from, E_α.

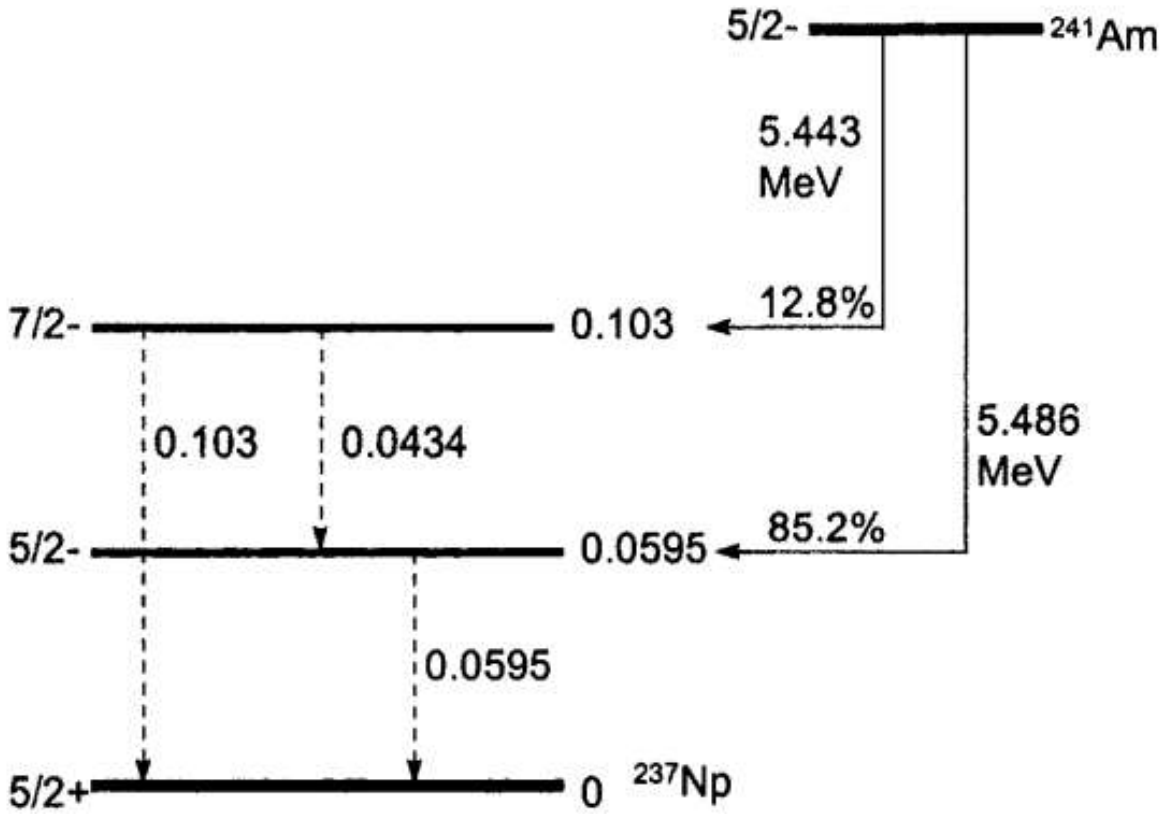

Fig.(1.5) Partial decay scheme of $^{241}Am \rightarrow {}^{237}Np$. The two principal α-particle energies are 5.486 MeV (85.2%) and 5.443 MeV (12.8%), both to excited states of the ^{237}Np daughter nucleus. The subsequent decay of the 0.0595 MeV state is by γ-emission to the ^{237}Np ground state. The α-energies not shown in the figure lie in the range 5.545 MeV to 4.800 MeV. ^{241}Am has a half-life of 433 yr.

1.3.4 Neutron (fission) decay

Certain of the actinide nuclei are capable of undergoing spontaneous (as opposed to induced) fission. They are also all α -particle emitters. As Table 1.2 shows, however, the probability of α-emission is always greater than the probability of spontaneous fission, although in ^{252}Cf the probabilities are much closer. Since there is in addition a greater neutron yield, ^{252}Cf is the isotope of choice for the production of a fission neutron spectrum.

All neutron-emitting sources are encapsulated within a high-quality welded stainless steel container that has a thickness greater than the range of the most energetic a-particle. For high-activity sources the energy deposited into the walls of the container will result in a perceptible rise in temperature.

Table (1.2) Some spontaneous fission neutron sources

Nuclide	α-emission half-life	n-emission half-life	neutron per fission	neutron $mg^{-1}\ s^{-1}$
^{242}Cm	162.8 d	6.1×10^{6} yr	2.3	1.7×10^{4}
^{244}Cm	18.1 yr	1.35×10^{7} yr	2.6	9×10^{3}
^{252}Cf	2.64 yr	82.5 yr	3.5	2.7×10^{9}

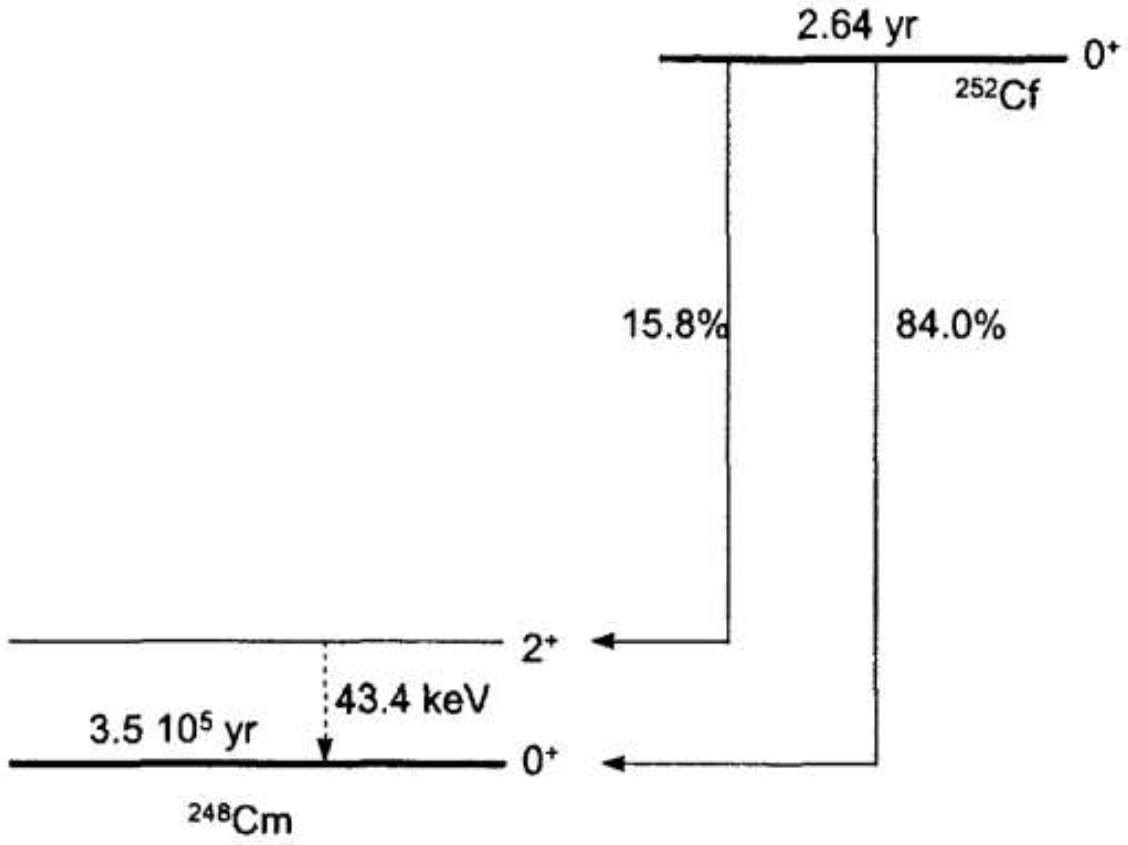

Fig.(1.6) Principal decay scheme of ^{252}Cf. The α-particle energies are 6.118 MeV (84%) and 6.076 MeV (15.8%).

An empirical expression [6] which gives the fraction $S(E)dE$ of fission neutrons with energy in the range between E and $E+dE$ is :

$$S(E) = 0.771\sqrt{E}\,\exp(-0.776 \times E) \tag{1.12}$$

This is normalized to unity such that :

$$\int_0^\infty S(E)dE = 1$$

and plotted in Fig.(1.7). The mean energy of the distribution, Eq.(1.13), has a value of 1.93 MeV.

$$\overline{E} = \frac{\int_0^\infty E\ S(E)\ dE}{\int_0^\infty S(E)\ dE} \tag{1.13}$$

1.4.2 *Van de Graaff generator*

The electrostatic charging of a metallic sphere takes place by means of two sets of corona points (a "comb" made of small diameter wires). One of these is at ground potential and the other is inside the high voltage terminal. To achieve a positive terminal potential the corona points at ground potential have one end connected to the positive terminal of a dc power supply. The other end has sharp points which lightly touch a flexible insulating belt, the purpose of which is to carry the charges up the potential gradient to the high voltage terminal. Inside the terminal the corona points are also in light contact with the belt and are connected to the spherical terminal through a large resistor R.

If the charging current carried upwards by the belt into the terminal (capacitance C with respect to ground) is dq/dt C s^{-1}, then the rate of increase of terminal potential is :

$$\frac{dV}{dt} = \frac{1}{C}\frac{dq}{dt}$$

The capacitance of a sphere of radius r is $C = 4\pi\varepsilon_0 r$. In SI units, C is in Farads, r in

metres and ε_0, the permittivity of free space, is 1.11×10^{-10} Fm^{-1}.

For practical reasons, the terminal must be enclosed within an outer sphere, radius R. In this case, the capacitance to ground becomes, [7] :

$$C = 1.11 \times 10^{-10} \frac{R\,r}{R - r}$$

For R = 1 m, r = 0.5 m and a charging current of 0.5 mA, dV/dt is 4.5 MV s^{-1}.

This acceleration method can be used with either positive or negative terminal potentials. For electron acceleration, the terminal voltage is generally lower than for positive ions, but the available beam current is generally higher.

Electrical breakdown

The electric field on the surface of the inner sphere, V/r, will be in the order of MV m^{-1}. If this exceeds the breakdown strength of the medium surrounding the

sphere, electrical discharge and loss of terminal voltage will result. Even dry air at atmospheric pressure has a breakdown strength in the MV m^{-1} region.

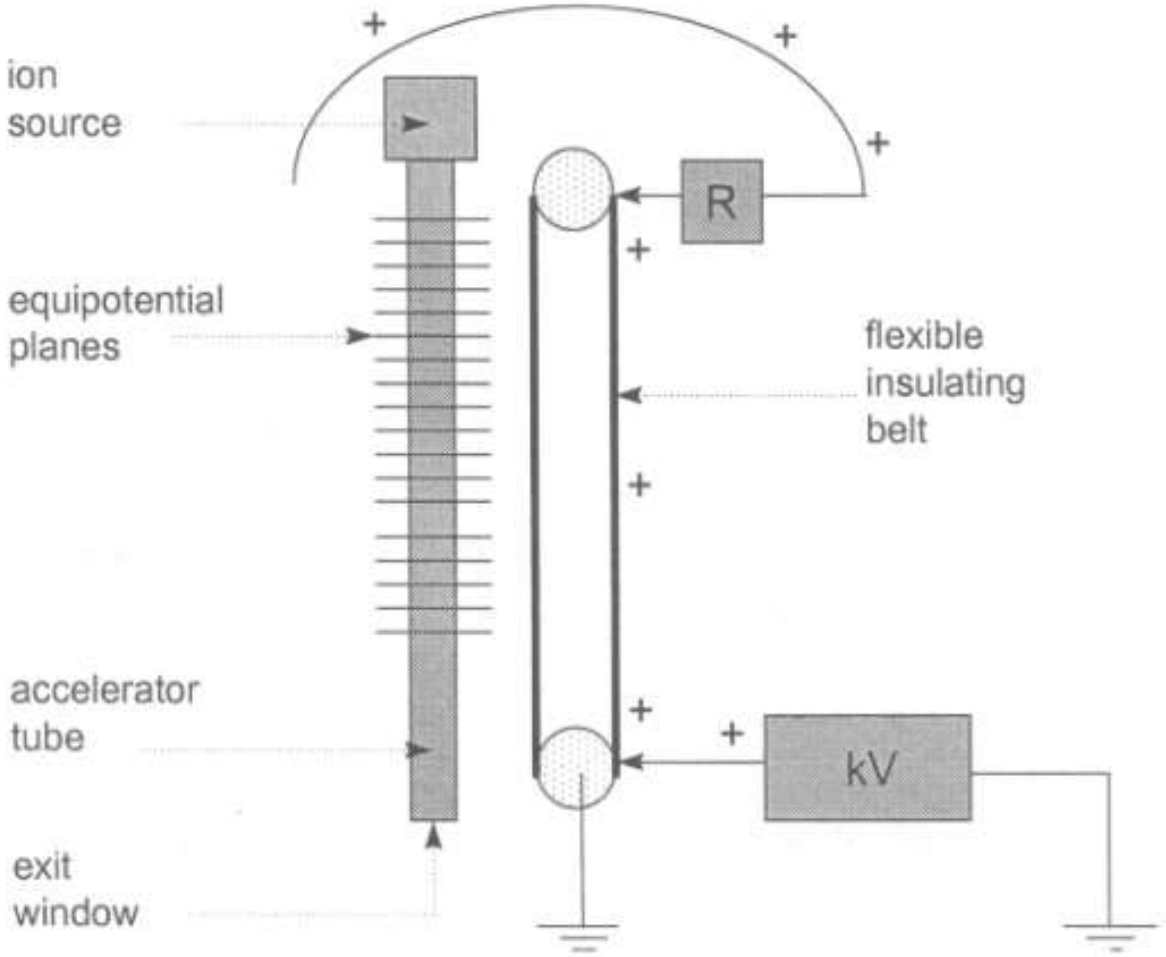

Fig.(1.9) The main features of a Van de Graaff generator. Corona points connected to the positive terminal of a dc power supply attract negative charge from a flexible insulating belt, rendering it positive. Because the belt is insulating, the charges remain in place and are carried upwards towards a similar set of corona points in the centre of a hollow metallic terminal sphere. These excess charges are neutralized by electrons drawn from the sphere which then becomes positively charged. The reverse process takes place as the belt moves downwards towards ground potential.

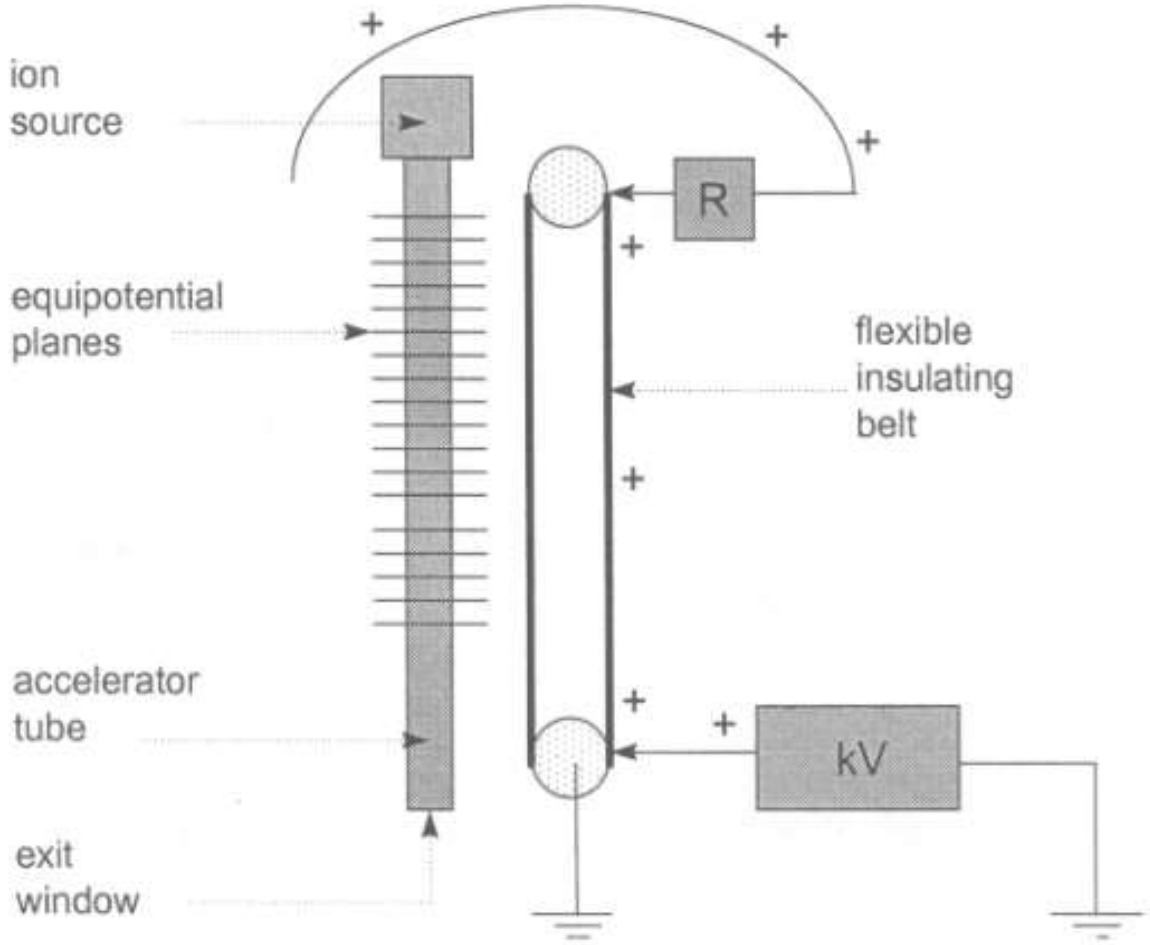

Fig.(1.9) The main features of a Van de Graaff generator. Corona points connected to the positive terminal of a dc power supply attract negative charge from a flexible insulating belt, rendering it positive. Because the belt is insulating, the charges remain in place and are carried upwards towards a similar set of corona points in the centre of a hollow metallic terminal sphere. These excess charges are neutralized by electrons drawn from the sphere which then becomes positively charged. The reverse process takes place as the belt moves downwards towards ground potential.

Electron loading

The accelerator tube consists of a series of conducting rings (generally aluminium) that are separated by high quality quartz insulators. High value resistors (~1 – 2 MΩ) across successive rings maintain a uniform potential drop from the terminal voltage to ground. Since there is no opportunity for beam focusing during the acceleration stage, the accelerated particles can strike the sides of the accelerator tube and release secondary electrons.

Tandem acceleration

In a conventional single-stage accelerator, the ion source is located within the high voltage terminal. Particles can be accelerated to double the terminal potential (although with much less efficiency) by using certain techniques of adding electrons to, and then stripping electrons from, an ion.

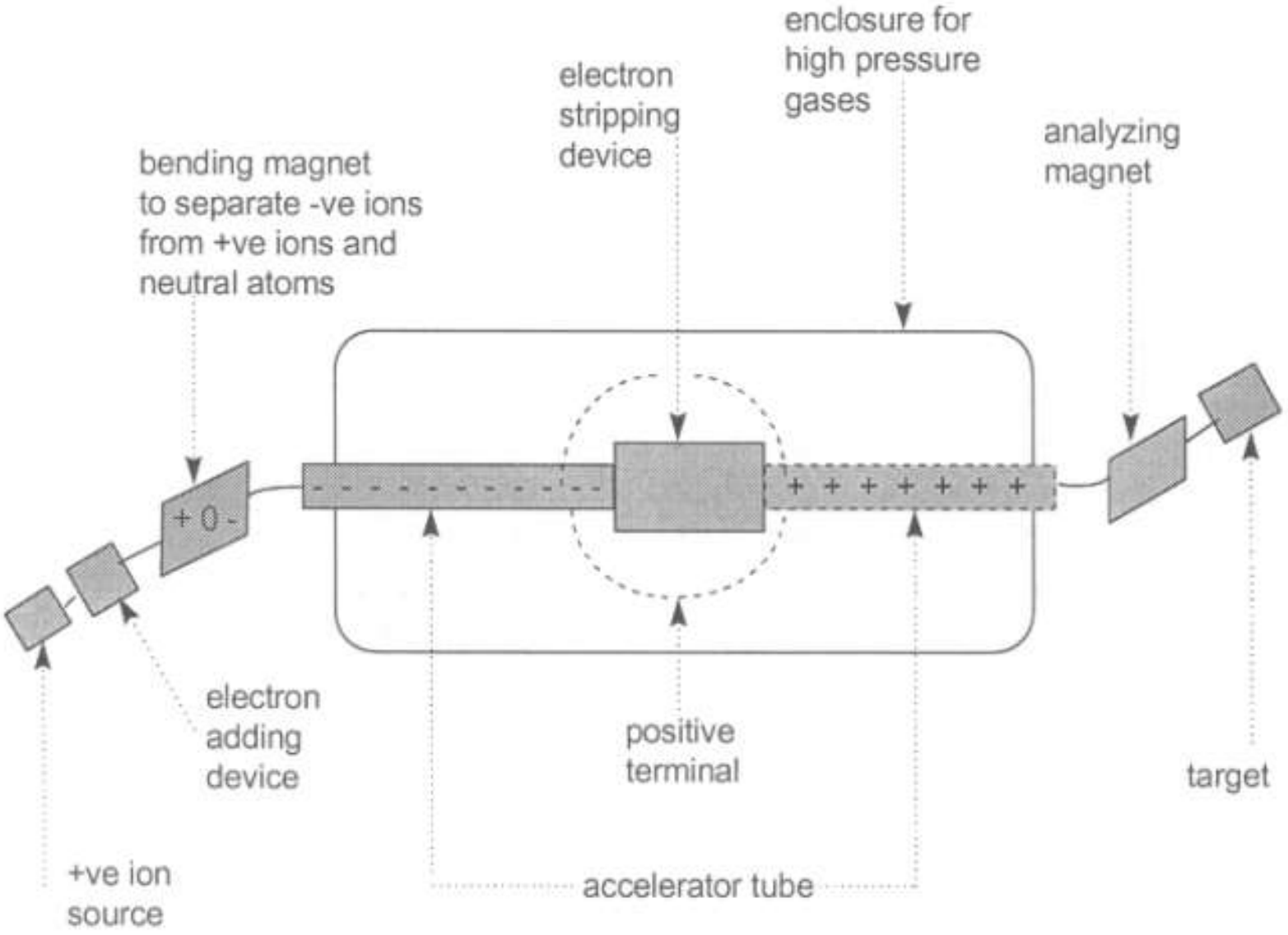

Fig.(1.11) A schematic diagram of the tandem Van de Graaff principle, [7].

1.4.3 *Cyclotron*

A conventional cyclotron uses resonance radio-frequency (rf) acceleration of heavy charged particles in a uniform dc magnetic field. This is achieved by placing an ion source at the centre of two "D"-shaped semicircular, hollow electrodes. The rf field is applied across the electrodes such that each "D" goes alternately positive and negative at the rf frequency, f_0. The cyclotron can only be used to accelerate heavy ions (p, d, He, H^- ....).

The motion of a particle of mass m and charge ze having velocity v, moving in a magnetic induction *B* with radius r, is governed by the Lorentz and centripetal forces.

$$B\ ze\ v = m\frac{v^2}{r} \tag{1.15}$$

The total energy *E* of the particle having kinetic energy *T*, is :

$$E = T + W_0 = T + m_0c^2 = mc^2 = \frac{m_0c^2}{\sqrt{\left(1-\beta^2\right)}} \tag{1.16}$$

where W_0 is the rest energy of the particle and $\beta = v/c$. Using Eqs.(1.15) and (1.16), the orbital frequency of the ion can be written :

$$f_i = \frac{v}{2\pi r} = \frac{ze\,B}{2\pi m} = \frac{ze\,B\,c^2}{2\pi(W_0 + T)} \qquad (1.17)$$

The resonance acceleration can be maintained only for a constant frequency, f_0. Since the kinetic energy of the particle increases with each crossing of the gap, the condition $f_i = f_0$ is only possible if $T << W_0$, *i.e.* at low energies.

A positive ion which emerges from the source in Fig.(1.12) is accelerated when the right-hand D is in the negative half cycle. There is no accelerating field within the hollow D so the particle experiences only the magnetic field. The particle follows a semicircular path until it reaches the edge of the D. If the time to traverse this path is the same as the time necessary for the left-hand D to become negative, the acceleration process will continue. For continuous acceleration the phase of the rf field must be slightly ahead of the phase at which the particle crosses the gap. This is the resonance condition.

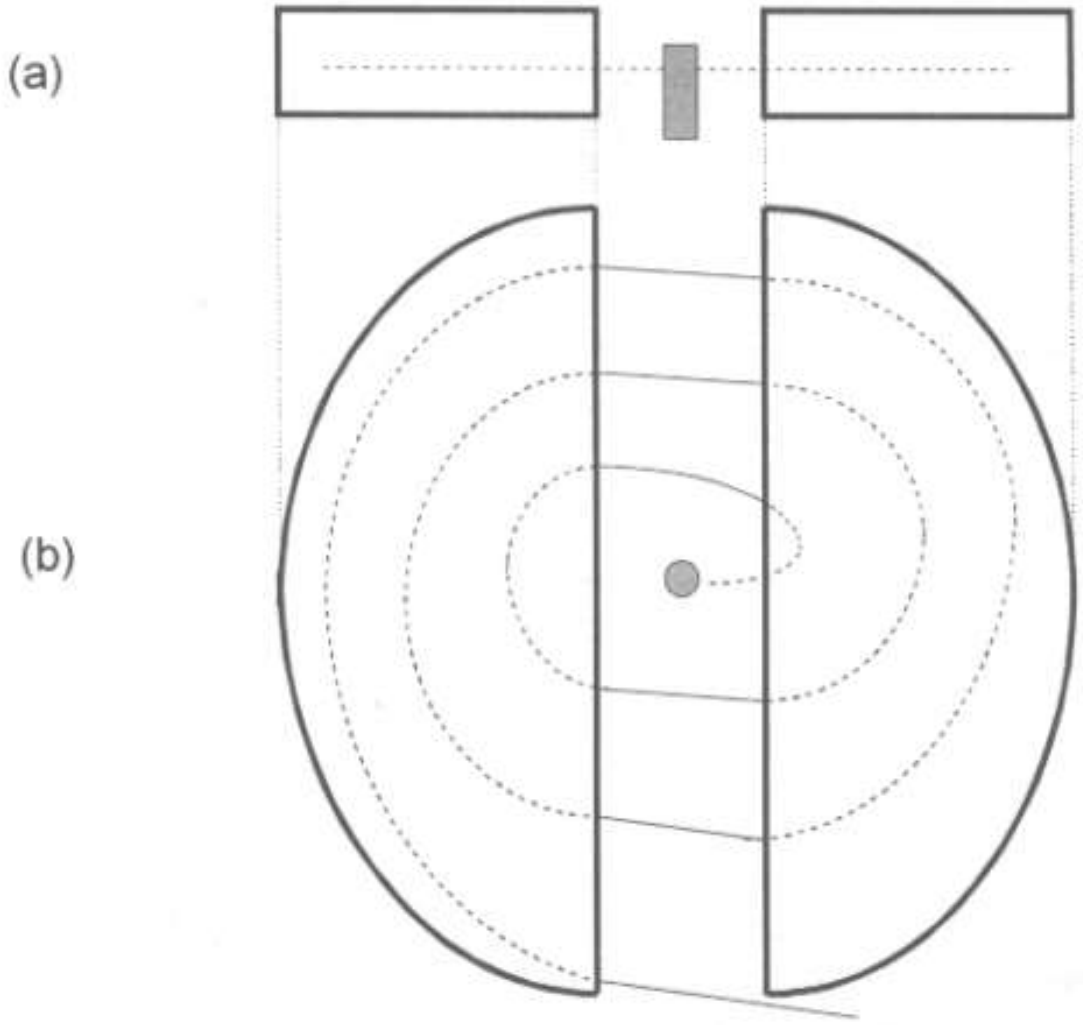

Fig.(1.12) Schematic diagram of the "D" structure of a cyclotron. (a) cross section (b) plan view. The ion source is at the centre and the dc magnetic field lines are perpendicular to the plane of the diagram, [7].

Weak-focusing

The requirement is that the lines of magnetic induction are always concave inwards towards the centre of revolution of the ions. This is achieved by the introduction of shim material, Fig.(1.13), in the central regions of the field together with the shaping of the pole pieces at the extremities of the field.

To set up the condition of weak-focusing, the magnetic induction B_o at a final orbit radius of r_o is first specified. At any other radius, r, the magnetic induction must then be given by :

$$B = B_0\left(\frac{r_0}{r}\right)^n$$

where $0<n<1$ for particles travelling near the final orbit radius. The consequence of this restoring force is that there are oscillations of the ion in both radial and axial di

di

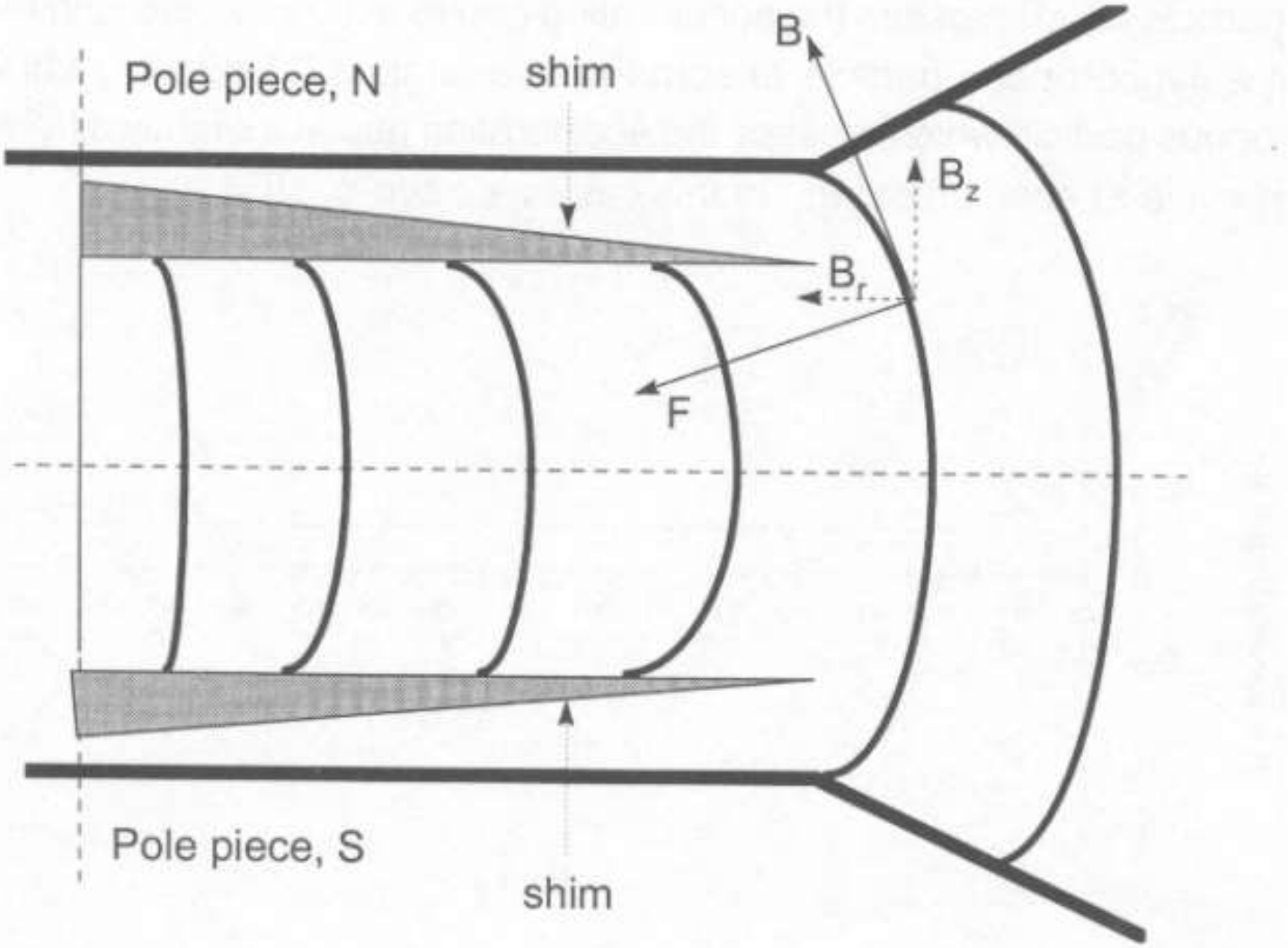

Fig.(1.13) Lines of magnetic induction in a weak-focusing field. A particle which is not travelling on the central plane will experience a force F which always tends to restore it into the central plane. This has an axial component F_z towards the central plane and a radial component F_r towards the centre of revolution, [7].

These oscillations have frequencies, [7] :

$$\text{Axial: } f_z = n^{1/2} f_i$$

$$\text{Radial: } f_r = (1-n)^{1/2} f_i$$

and are always smaller than the ion frequency, hence the name 'weak-focusing'. The overriding requirement is that the magnetic induction decreases as the radius increases.

Phase stability

The above requirement for weak-focusing is not consistent with the resonance

condition in Eq.(1.17). As T becomes significant with respect to W_0 the ion frequency f_i decreases. In order to maintain the resonance condition in a constant magnetic field, either :

- the rf frequency f_0 must also decrease or,
- if f_0 remains constant, B must increase as r increases. Certainly it cannot decrease, as in weak-focusing.

Van de Graaff generator

A Van de Graaff generator is an electrostatic generator which uses a moving belt to accumulate very high amount of electrical potential on a hollow metal globe on the top of the stand.

It was invented by American physicist Robert J. Van de Graaff in 1929.

The potential difference achieved in modern Van de Graaff generators can reach 5 megavolts. A tabletop version can produce on the order of 100,000 volts and can store enough energy to produce a visible spark.

A Van de Graaff generator operates by transferring electric charge from a moving belt to a terminal.

The "high voltages generated by the Van de Graaff generator can be used for accelerating subatomic particles to high speeds, making the generator a useful tool for fundamental physics research.

Van de Graaff Generator

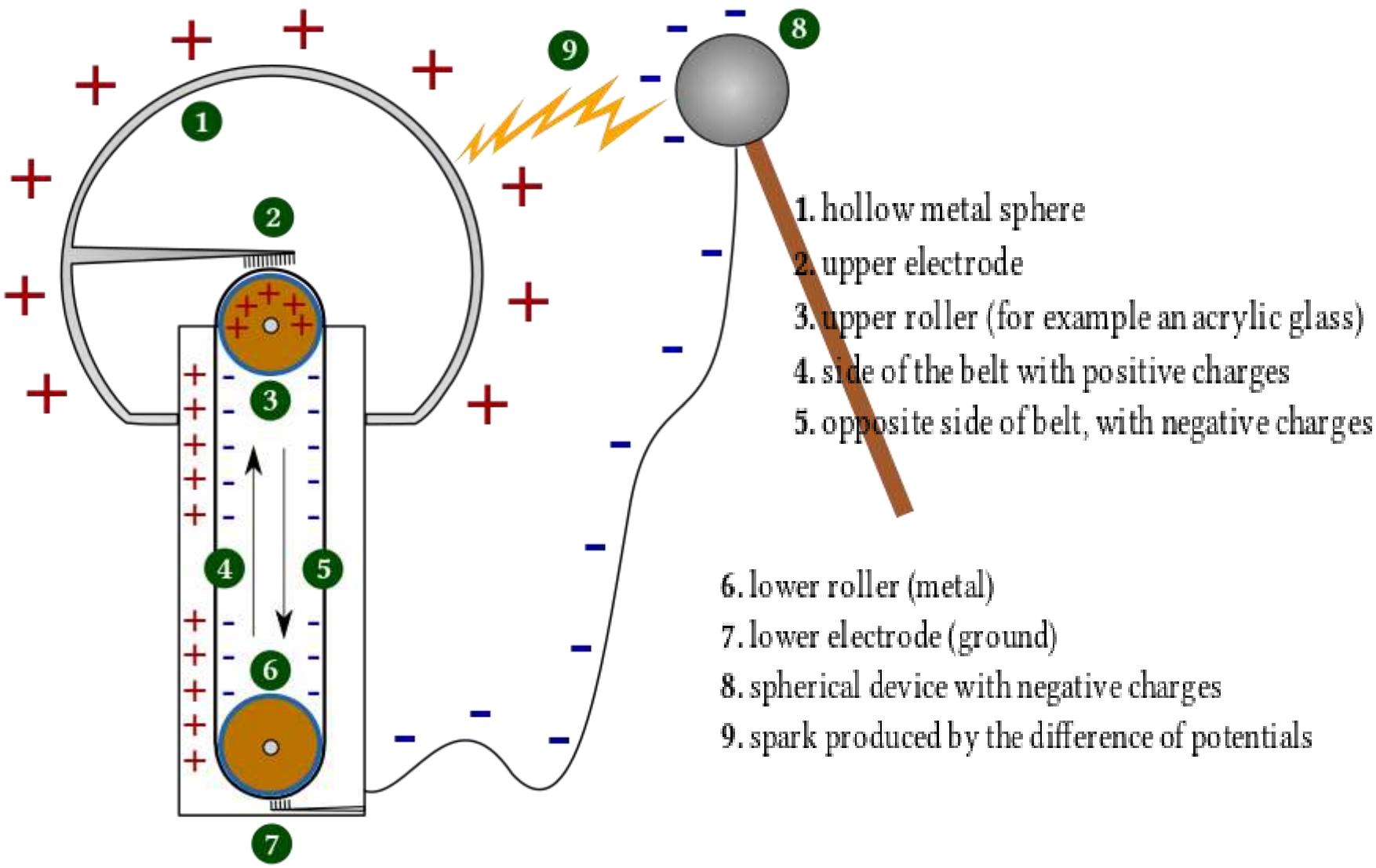

1. hollow metal sphere
2. upper electrode
3. upper roller (for example an acrylic glass)
4. side of the belt with positive charges
5. opposite side of belt, with negative charges
6. lower roller (metal)
7. lower electrode (ground)
8. spherical device with negative charges
9. spark produced by the difference of potentials

A simple Van de Graaff-generator consists of a belt of silk, or a similar flexible dielectric material, running over two metal pulleys, one of which is surrounded by a hollow metal sphere. Two electrodes, (2) and (7), in the form of comb-shaped rows of sharp metal points, are positioned respectively near to the bottom of the lower pulley and inside the sphere, over the upper pulley.

Comb (2) is connected to the sphere, and comb (7) to the ground. A high DC potential (with respect to earth) is applied to roller (3): a positive potential in this example.

As the belt passes in front of the lower comb, it receives negative charge that escapes from its points due to the influence of the electric field around the lower pulley, which ionizes the air at the points.

As the belt touches the lower roller (6), it transfers some electrons, leaving the roller with a negative charge (if it is insulated from the terminal), which added to the negative charge in the belt generates enough electric field to ionize the air at the points of the upper comb. Electrons then leak from the belt to The upper comb and to the terminal, leaving the belt positively charged as it returns down and the terminal negatively charged.

The sphere shields the upper roller and comb from the electric field generated by charge that accumulate at the outer surface of it, causing the discharge and change of polarity of the belt at the upper roller to occur practically as if the terminal were grounded.

As the belt continues to move, a constant charging current travels via the belt, and the sphere continues to accumulate negative charge until the rate that charge is being lost (through leakage and corona discharges) equals the charging current. The larger the sphere and the further it is from ground, the higher will be its final potential.

Another method for building Van de Graaff generator is to use the triboelectric effect. The friction between the belt and the rollers, one of them now made of insulating material, or both made with insulating materials at different positions on the triboelectric scale, one above and other below the material of the belt, charges the rollers with opposite polarities.

The strong e-field from the rollers then induces a corona discharge at the tips of the pointed comb electrodes. The electrodes then spray a charge onto the belt which is opposite in polarity to the charge on the rollers.

The remaining operation is otherwise the same as the voltage-injecting version above. This type of generator is easier to build for science fair or homemade projects, since it does not require a potentially dangerous high-voltage source. Finally, since the position of the rollers can be reversed, the accumulated charge on the hollow metal sphere can either be positive or negative.

A Van de Graaff generator terminal does not need to be sphere-shaped to work, and in fact, the optimum shape is a sphere with an inward curve around the hole where the belt enters.

Since electrically charged conductors have no e-field inside, charges can be added continuously. A rounded terminal minimizes the electric field around it, allowing greater potentials to be achieved without ionization of the surrounding air, or other dielectric gas.

Since a Van de Graaff generator can supply the same small current at almost any level of electrical potential, it is an example of a nearly ideal current source. The maximum achievable potential is approximately equal to the sphere's radius multiplied by the e-field where corona discharge begin to form within the surrounding gas.

For example, a polished spherical electrode 30 cm in diameter immersed in air at STP (which has a breakdown volt age of about 30 kV/cm) could be expected to develop a maximum voltage of about 450 kV.

A more recent development is the tandem Van de Graaff accelerator, containing one or more Van de Graaff generators, in which negatively charged ions are accelerated through one potential difference before being stripped of two or more electrons, inside a high voltage terminal, and accelerated again.

An example of a three stage operation has been built in Oxford Nuclear Laboratory in 1964 of a 10 MV single-ended “injector” and a 6 MV EN tandem.

The Nuclear Structure Facility (NSF) at Daresbury Laboratory was proposed in the 1970s, commissioned in 1981, and opened for experiments in 1983. It consisted of a tandem Van de Graaff generator operating routinely at 20 MV, housed in a distinctive building 70 metres high. During its lifetime, it accelerated 80 different ion beams for experimental use, ranging from protons to uranium.

A particular feature was the ability to accelerate rare isotopic and radioactive beams. Perhaps the most important discovery made on the NSF was that of super deformed nuclei. Thesis nuclei, when formed from the fusion of lighter elements, rotate very rapidly. The pattern of gamma rays emitted as they slow down provided detailed information about the inner structure of the nucleus. Following financial cutbacks, the NSF closed in 1993.